

Morphology, interfacial electronic structure, and optical properties of oligothiophenes grown on ZnSe(100) by molecular beam deposition

S. Blumstengel,¹ N. Koch,¹ S. Duhm,¹ H. Glowatzky,¹ R. L. Johnson,² C. Xu,¹ A. Yassar,³ J. P. Rabe,¹ and F. Henneberger¹

¹*Institut für Physik, Humboldt-Universität zu Berlin, Newtonstrasse 15, 12489 Berlin, Germany*

²*Institut für Experimentalphysik, Universität Hamburg, 22761 Hamburg, Germany*

³*CNRS, ITODYS, Université Paris 7, 1 rue Guy de la Brosse, 75005 Paris, France*

(Received 12 January 2006; published 20 April 2006)

We report on the growth of two types of oligothiophenes, α -sexithiophene and a substituted terthiophene, on $c(2 \times 2)$ reconstructed ZnSe(100) surfaces by molecular beam deposition. The study is aimed at a deeper understanding of the structural and electronic properties of organic/inorganic semiconductor interfaces. The structure and morphology of the organic adlayer from submonolayer up to several monolayer coverage were characterized by atomic force microscopy. The interfacial electronic structure and the optical properties were investigated by photoemission and photoluminescence spectroscopy, respectively. The results reveal that the organic adlayer is bonded by van der Waals forces to the ZnSe(100) $c(2 \times 2)$ surface. The electronic structure and the optical properties of the two materials forming the interface remain unperturbed, indicating that surface passivation, which is found indispensable when using other covalent inorganic semiconductor surfaces such as GaAs as substrates for organic thin films, is not required to allow for an ordered growth of the organic adlayer on ZnSe(100).

DOI: [10.1103/PhysRevB.73.165323](https://doi.org/10.1103/PhysRevB.73.165323)

PACS number(s): 79.60.Jv, 78.66.Qn, 78.68.+m, 79.60.Fr

INTRODUCTION

Organic semiconductors attract great attention as an alternative to the more conventional inorganic materials for application in optoelectronic devices.^{1,2} However, as both material classes have their own advantages it appears interesting to combine organic and inorganic semiconductors to benefit from the favorable properties of both material classes. For example, the high charge-carrier mobilities inherent in the inorganic layer could be linked with the large oscillator strength and facile tunability of optical absorption and emission of the organic material. One approach consists in the combination of organic materials with epitaxial semiconductor nanostructures. This might lead to a class of new light-emitting or photovoltaic devices in which phenomena such as charge or energy transfer at the organic/inorganic interface could be exploited. To this end, a profound understanding of the organic-inorganic interface is essential. This regards the structure and morphology as well as the electronic properties of the interface. Charge and energy transfer should sensitively depend on the orientation of the molecules with respect to the substrate surface while the arrangement of the molecules within the organic layer and the lateral size of the crystalline domains determine luminescence properties. The native unreconstructed surface of a covalent semiconductor exhibits usually a large density of dangling bonds. If molecules are in contact with such a surface, the electronic structure of the inorganic semiconductor and that of the molecules in the organic adlayer may be altered due to chemical bond formation which, in turn, affects charge or energy transfer processes at the interface. Moreover, bond formation should affect the ordering of the organic adlayer. In an early study on the growth of 3,4,9,10-perylenetetracarboxylic dianhydride deposited on GaAs(001) with different surface reconstructions, it was found that the dangling bonds

increase the pinning of the molecules at the interface leading to structural disorder in the organic film.³ An ordered growth was only achieved after passivation of the surface with selenium or sulfur, eliminating the chemically active sites and, thus, weakening the molecule-surface interaction.^{3,4}

In the above context, ZnSe and related compounds should be especially interesting as they have band gaps tunable in the range of 1.5–3.0 eV and thus match well the gap between the highest occupied molecular orbital (HOMO) and the lowest unoccupied molecular orbital (LUMO) of many organic conjugated materials including oligothiophenes. The growth and structural and electronic properties of organic layers deposited on this semiconductor surface have not been studied up to now, while photoluminescence and infrared spectroscopic studies of oligothiophenes on ZnSe have been performed.^{5,6}

We report here about the growth of two types of oligothiophenes, α -sexithiophene and a substituted terthiophene, namely, 4,4''-dicyano-3',4'-ethylenedioxy-2,2':5,2''-terthiophene, on $c(2 \times 2)$ reconstructed ZnSe(100) surfaces. We have chosen oligothiophenes as they represent well-studied model compounds.⁷ To understand the intrinsic properties of organic-inorganic interfaces, it is indispensable to prepare the organic adlayer on a well-defined, atomically flat, and chemically clean semiconductor surface in a controlled manner and under ultraclean conditions. Therefore we employed molecular beam deposition as the entire structure can be prepared under ultrahigh-vacuum (UHV) conditions without exposure to ambient atmosphere.

As we are especially interested in the interface properties, we prepared ultrathin films ranging from submonolayers up to several layers. Their morphology was investigated by atomic force microscopy (AFM). The interfacial electronic structure was characterized by combined ultraviolet and x-ray photoelectron spectroscopy. In order to check if the

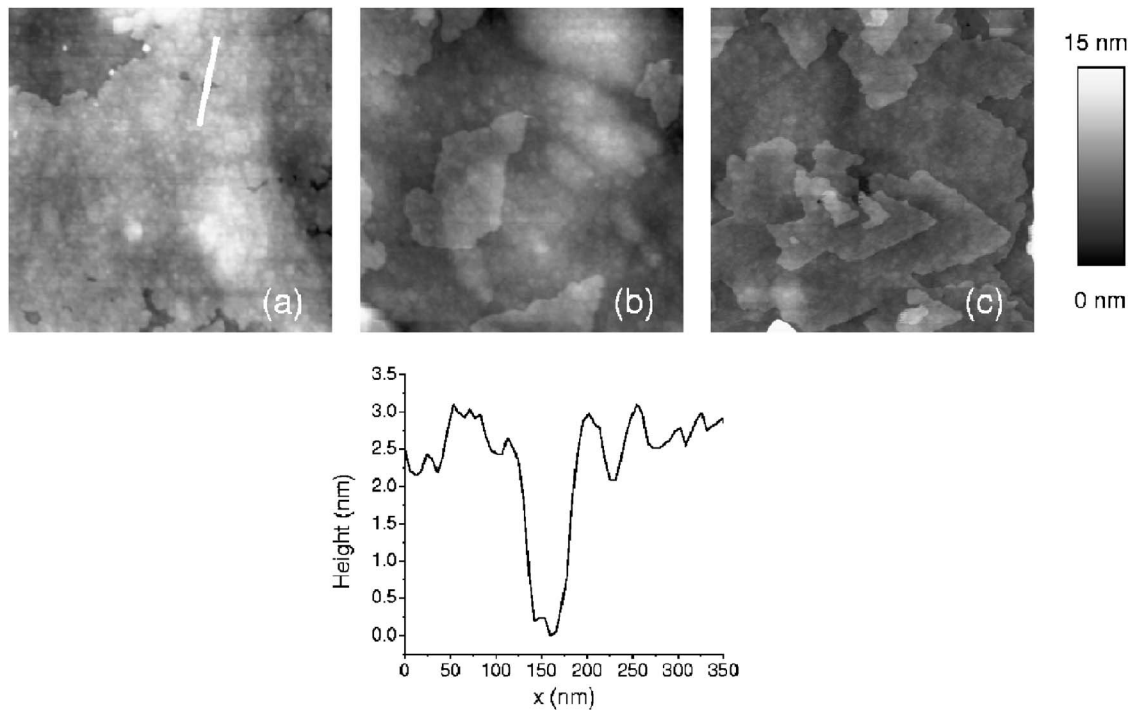


FIG. 1. AFM images of 6T on ZnSe(100) kept at 373 K during the deposition of the organic layer. The layer thicknesses are 1.6 (a), 2.5 (b), and 5 nm (c). The scan area is $1.5 \times 1.5 \mu\text{m}^2$. The height profile was taken along the white line.

optical properties of the organic layer were modified when in contact with the inorganic semiconductor surface, photoluminescence (PL) spectroscopy was employed.

EXPERIMENT

ZnSe epilayers with a thickness of $1 \mu\text{m}$ were grown on (001)-oriented GaAs by molecular beam epitaxy.⁸ To protect the surface against oxidation, the epilayers were capped with an amorphous selenium layer. α -sexithiophene (6T) (Aldrich) and 4,4''-dicyano-3',4'-ethylenedioxy-2,2':5,2''-terthiophene⁹ (CN-3T) (chemical structure see Fig. 6) were deposited in a second growth chamber with a base pressure of 1.5×10^{-9} Torr from Knudsen-type effusion cells (DCA Instruments) after thermal removal of the selenium layer. The desorption process was monitored by reflection high-energy electron diffraction and stopped when the $c(2 \times 2)$ surface reconstruction became visible. The thickness of the organic layers was measured with a quartz microbalance. All reported thickness values represent nominal thicknesses as they were not corrected with the respective sticking coefficients on ZnSe. The substrate temperature was chosen between 263 and 373 K while the deposition rate was kept constant at $1 \text{ \AA}/\text{min}$. The morphology of the deposited organic layer was investigated *ex situ* by AFM in tapping mode (Digital Instruments). PL spectra were recorded with a cooled charge-coupled device matrix coupled to a monochromator. The samples were placed in a helium flow cryostat and excited by a dye laser tunable between 435 and 465 nm which was pumped by an Ar^+ laser.

Photoemission experiments were performed at the FLIPPER II end station at HASYLAB (Hamburg, Germany),

comprised of interconnected preparation and analysis chambers. The base pressure in the chambers was 2×10^{-9} and 2×10^{-10} mbar, respectively. Se-capped ZnSe epilayers were annealed in UHV for several minutes to produce a $c(2 \times 2)$ reconstructed surface as verified by low-energy electron diffraction. Subsequently, 6T as well as CN-3T were evaporated in UHV from resistively heated pinhole sources, at a rate of ca. 2 \AA per minute. Photoemission spectra were recorded for the pristine $c(2 \times 2)$ ZnSe surfaces, and for stepwise-increasing thicknesses of the organic adlayer. Valence electron spectra were recorded with a photon energy of 22 eV, and Zn 3d and Se 3d core level spectra with 80 eV. For recording secondary-electron cutoff spectra, the samples were biased at -5 V . The energy resolution of the electron spectrometer was set to 0.15 eV. The overall error of the values derived from photoemission experiments is estimated with $\pm 0.1 \text{ eV}$.

RESULTS AND DISCUSSION

Morphology

Figure 1 displays AFM images of 6T with nominal layer thicknesses of 1.6, 2.5, and 5 nm deposited on ZnSe(100) at a substrate temperature of 373 K. From Fig. 1(a) as well as from scans taken over larger areas (not shown here) it is evident that before nucleation of a second layer sets in, an almost complete monolayer of 6T is formed. The thickness of the first layer is ca. 2.5 nm which corresponds approximately to half of the c -lattice constant of the 6T crystal. Thus the contact plane of the 6T crystal should be the (001) crystal plane. However, taking into account the experimental error,

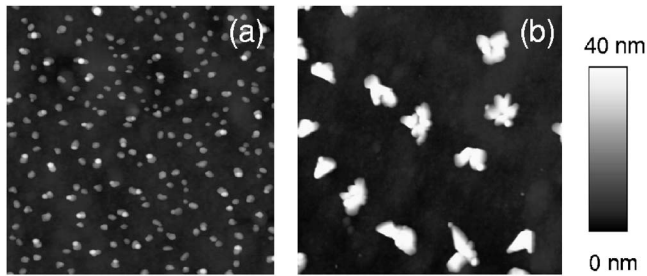


FIG. 2. AFM images of CN-3T on ZnSe(100). (a) Substrate temperature 263 K, layer thickness 1 nm; (b) substrate temperature 298 K, layer thickness 3 nm. The scan area is $3.0 \times 3.0 \mu\text{m}^2$.

it is not possible to decide whether 6T molecules assemble as in the bulk (long molecular axes form an angle of 23° with respect to the c crystal axis)¹⁰ or as in the thin film phase found, for instance, on silicon dioxide substrates (molecules are parallel to the c axis).^{11–13} The assembly of the molecules is determined by the balance of the interaction energy of 6T with the substrate surface and the intermolecular interaction energy which is, considering the shape of the molecule, highly anisotropic. For an isolated molecule it should be energetically more favorable to lie flat on the surface. Recently reported confocal laser scanning microscopy PL images of 6T on SiO_2 with submonolayer coverage confirm such a behavior.¹⁴ Similar to the case of pentacene,¹⁵ the (001) plane of the 6T crystal should exhibit the lowest surface energy. Thus, in order to minimize the surface energy, molecules should orient upright in the islands provided that the interaction energy between molecules and substrate is weaker than the intermolecular interaction. Judging from AFM data, this is indeed the case for the ZnSe/6T interface. Continuing the deposition, the growth proceeds in a layered mode whereby a new layer starts to nucleate before completion of the underlying layer [Figs. 1(b) and 1(c)] pointing to Stranski-Krastanov-type growth. In Fig. 1(c) the formation of facets is clearly seen. The facet angle [Fig. 1(c)] is close to that between the $(\bar{1}10)$ and (110) crystallographic directions. This means that 6T molecules diffusing across the surface and reaching step edges are not immobilized, and on the time scale of deposition, transport between different step facets to energetically more favorable sites occurs. The growth velocity of terraces is thus dependent on the orientation of the step edges. Since the edges of the facets of superimposed layers are mostly parallel it can be concluded that the domains are monocrystalline. However, no preferential orientation of the crystalline domains with respect to the crystallographic directions of the ZnSe substrates was found.

A quite different film morphology is observed for CN-3T. In Fig. 2, AFM images are reported for growth temperatures of 263 and 298 K and layer thicknesses of 1 and 3 nm, respectively. The AFM images reveal the formation of three-dimensional (3D) islands, in contrast to the predominantly two-dimensional terracelike morphology found for 6T on ZnSe(100) also at room temperature (AFM data not shown here). Whether or not an ultrathin wetting layer is present could not be determined by AFM measurements. However, photoemission data which will be discussed in the next sec-

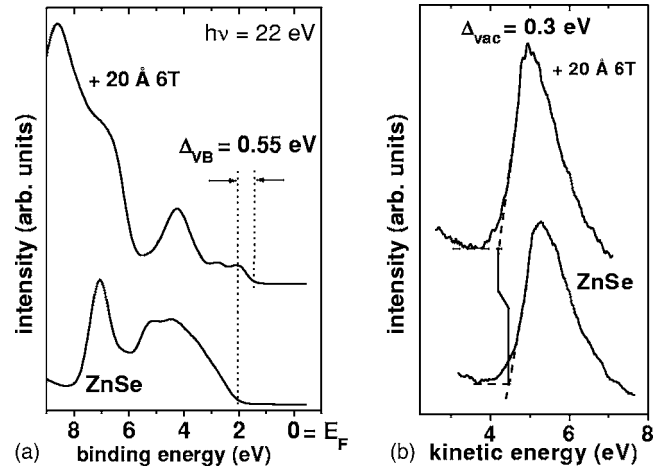


FIG. 3. (a) Valence region photoemission spectra of ZnSe $c(2 \times 2)$ (bottom) and with 20 Å 6T coverage. (b) Corresponding secondary-electron cutoff spectra.

tion hint at the presence of such a layer. The shape of the nuclei depends on the surface energies of the crystal and the interfacial energy on ZnSe. The crystal structure of CN-3T in the bulk can be pictured as a slipped π - π stack structure.⁹ It is quite different from the herringbone structure adopted by 6T. Thus it is not surprising that the film morphologies of CN-3T and 6T on ZnSe(100) are different under comparable growth conditions. A more quantitative analysis is not possible as the crystal structure of CN-3T in the thin film phase, the contact planes, the adhesion energies as well as the vapor pressure of the material are not known. However, Figs. 2(a) and 2(b) show that the density of the 3D islands decreases with increasing growth temperature suggesting a diffusion-mediated growth process.

Interfacial electronic structure

The valence electron photoemission spectrum of the $c(2 \times 2)$ ZnSe surface (bottom curve in Fig. 3) exhibits an energy separation between the valence band edge and the Fermi energy (E_F) of 2.0 eV. The deposition of 6T leads to an attenuation of photoemission intensity from the ZnSe valence band, and distinct features derived from 6T molecular orbitals become visible. At a nominal 6T coverage of ca. 20 Å only these dominate the spectrum (see top curve in Fig. 3). The energy levels of 6T are essentially flat away from the interface, as inferred from thickness-dependent measurements (not shown). Features centered at binding energies (BEs) of 2.0 eV and 2.7 eV correspond to the 6T HOMO and HOMO-1, respectively. The overall spectral shape reproduces that reported for thicker films very well.¹⁶ The BE onset of the HOMO is 1.45 eV below E_F . Consequently, the energy offset between the ZnSe valence band maximum (VBM) and the 6T HOMO onset is 0.55 eV. No indications for a chemical interaction between the ZnSe surface and 6T can be derived from valence photoemission spectra. This is in agreement with the observed morphology of the first deposited monolayers of 6T which is typical for weakly interacting substrates where intermolecular interactions are stron-

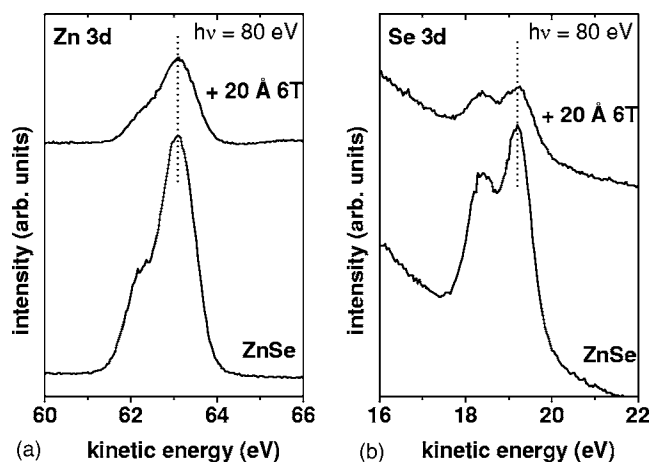


FIG. 4. (a) Zn $3d$ and (b) Se $3d$ core-level spectra for pristine ZnSe $c(2 \times 2)$, and after deposition of 20 \AA 6T.

ger than the substrate-adsorbate interaction. Upon adsorption of 6T, the sample work function (Φ) is reduced from 4.25 eV (pristine ZnSe) to 3.95 eV (20 \AA 6T, and more) as calculated from the change in kinetic energy of the secondary-electron cutoff [Fig. 3(b)].

Core-level photoemission spectra can also trace the bonding state of the surface and near-surface atoms of the ZnSe(100) substrate. Figures 4(a) and 4(b) display the Zn $3d$ and Se $3d$ photoemission spectra of the pristine ZnSe(100) $c(2 \times 2)$ surface (bottom) and after the evaporation of ca. 20 \AA 6T. The Zn $3d$ spectrum of the pristine sample consists of two components. The peak at 63 eV (corresponding to 10.8 eV BE) corresponds to the bulk atoms while the shoulder at 62 eV (high-BE side) can be attributed to a surface Zn $3d$ component.^{17–20} In the Se $3d$ spectrum of the pristine ZnSe surface, the contributions of the bulk and surface atoms cannot be resolved. Upon deposition of 6T, the intensity is attenuated of both the Zn $3d$ and the Se $3d$ spectra; however, energy positions and line shapes of these core levels remain unchanged. This is a clear indication that no chemical bond is formed between the surface atoms of ZnSe(100) and 6T. Therefore we conclude that the interaction is of van der Waals type.

A similar situation is found at the CN-3T/ZnSe $c(2 \times 2)$ interface. Upon stepwise deposition of CN-3T, photoemission peaks attributed to the molecule appear [Fig. 5(a)]. The top spectrum in Fig. 5(a) is a simulated UPS spectrum of CN-3T. It was obtained by Gaussian broadening (full width at half maximum 0.5 eV) of the molecular eigenenergies as obtained by semiempirical AM1 calculations.²¹ The theoretical spectrum corresponds well to the experimentally measured one, confirming that CN-3T adsorbs intact on the ZnSe surface. The photoemission peaks corresponding to the ZnSe valence bands become attenuated already for a nominal CN-3T coverage of 4 \AA . The energy positions of CN-3T valence emission features do not change with increasing layer thickness, indicating that band bending in the organic layer is absent and no changes in the electronic structure of the molecule occur (as in the case of 6T). From these spectra, the energy offset between the ZnSe VBM and the CN-3T HOMO onset can be determined to be 0.2 eV. Interestingly,

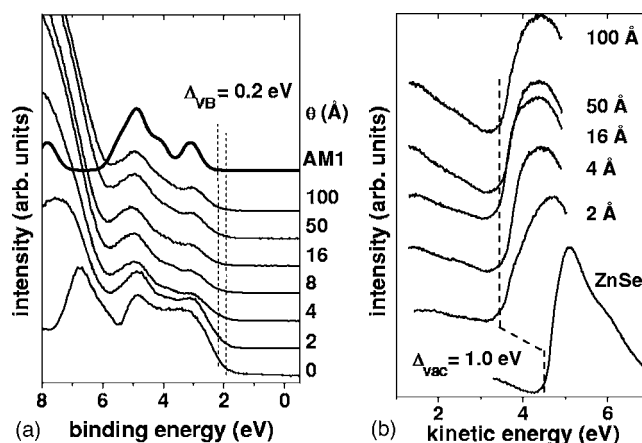


FIG. 5. (a) Valence region photoemission spectra of ZnSe $c(2 \times 2)$ and with increasing CN-3T thickness. (b) Corresponding secondary-electron cutoff spectra.

the secondary-electron cutoff exhibits a pronounced shift of 1 eV toward lower kinetic energy when going from the pristine ZnSe(100) surface to the CN-3T-covered surface [Fig. 5(b)]. The shift occurs almost entirely already at a nominal thickness of 2 \AA and remains constant for increasing layer thickness. This together with the observed damping of the ZnSe photoemission peaks at CN-3T coverages of 4 \AA hints at the formation of a wetting layer. Note that this information could not be obtained from AFM images. The change of work function (i.e., Φ) represents the vacuum level shift upon deposition of the organic adlayer. It is much larger than the value found at the ZnSe/6T interface. One reason for the reduction of Φ might be the modification of the surface dipole at the ZnSe $c(2 \times 2)$ surface upon deposition of the organic layer. Analogous examples exist for organic/metal interfaces.^{22,23}

In a II-VI semiconductor such as ZnSe, the cations and anions have two and six valence electrons, respectively, i.e., each atomic orbital contributes 1/2 and 3/2 electrons to each bond in the zinc-blende structure. Consequently, there are $2 \times 1/2$ and $2 \times 3/2$ electrons in the dangling bonds per cation or anion, respectively, in an unreconstructed surface. According to the electron counting rule, a dimer or a vacancy structure with a surface coverage of 1/2 can make the surface nonmetallic. After removing the Se capping layer, the ZnSe(100) surface displays a $c(2 \times 2)$ surface reconstruction. The structure of this surface can be most likely described by the Zn vacancy model. It consists of half a monolayer of Zn atoms on the (100) surface of the Se-terminated ZnSe bulk crystal.²⁴ The partially empty dangling bonds of the selenium atoms in the second layer accept electrons from the dangling bonds of the top zinc atoms and become fully occupied. This leads to the formation of a positive surface dipole.²⁰ Upon deposition of both organic materials, this surface dipole becomes larger. The much stronger increase of the surface dipole in the case of the CN-3T/ZnSe interface can be understood considering the chemical structure of the molecule (Fig. 6). As the cyano substituents are strongly electron withdrawing and the diethoxy group is electron donating, CN-3T possesses a large static dipole moment in the plane of the

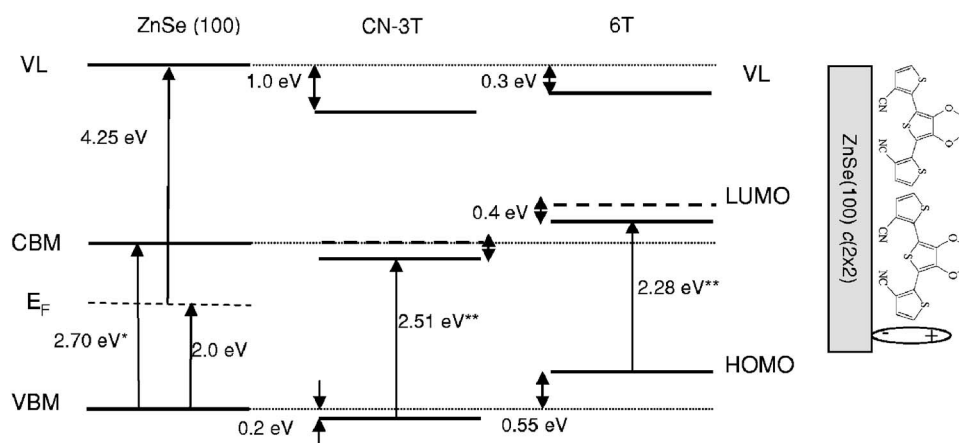


FIG. 6. Schematic energy-level diagrams of the 6T/ZnSe $c(2 \times 2)$ and CN-3T/ZnSe $c(2 \times 2)$ interfaces. The band gap of ZnSe (*) was taken from Ref. 17. The optical gaps at room temperature of 6T and CN-3T are indicated (**). The HOMO-LUMO gaps differ from those values by the exciton binding energy which amounts to approximately 0.4 eV in 6T according to Ref. 23. The calculated LUMO level of 6T is drawn by the dashed line. For CN-3T, the position of the LUMO level (dashed line) was estimated assuming a similar exciton binding energy as for 6T. Proposed arrangement of CN-3T molecules in the wetting layer.

molecule perpendicular to the long molecular axis. The CN-3T molecules in the wetting layer should consequently orient such that the cyano groups face the ZnSe surface (Fig. 6). Such an arrangement yields an additional resulting dipole moment that can explain the much stronger reduction of the vacuum level at the CN-3T/ZnSe interface in comparison to the 6T/ZnSe interface. As $c(2 \times 2)$ reconstruction makes the ZnSe surface semiconducting, it can be regarded as chemically relatively inert. This explains why the organic adlayers are bonded only by van der Waals forces. This finding is different from the behavior reported for other semiconductor surfaces. For example, photoelectron spectra of the interface between Si(100) (2×1) and pentacene reveal that a chemical bond is formed between the silicon dimers and the molecular π orbitals which results in a significant modification of the electronic structure of the first pentacene monolayer.²⁵

Figure 6 displays schematic energy-level diagrams of the 6T and CN-3T/ZnSe(100) interfaces derived from the photoemission spectra. Photoemission spectroscopy showed no electronic perturbations at both interfaces compared to the pure materials. The optical absorption gaps of the organics measured at room temperature are drawn in Fig. 6 as well. The HOMO-LUMO gaps differ from those values by the exciton binding energy. For 6T, the exciton binding energy was reported to be approximately 0.4 eV.¹⁶ With this value, the LUMO energy of 6T was calculated. Its position is displayed in Fig. 6. Consequently, the conduction band minimum (CBM)-LUMO off-set of the ZnSe/6T interface is approximately 0.53 eV. For CN-3T, the exciton binding energy is not known so far. Assuming a similar value, the CN-3T LUMO should approximately match the energetic position of the CBM of ZnSe.

Optical properties

The optical gaps of both 6T and CN-3T are smaller than the optical gap of ZnSe and there is spectral overlap of the respective absorption and emission spectra to allow for exci-

ton transfer via dipole-dipole interaction from ZnSe to the organic adlayer. This process should, however, be highly unlikely due to the negligible exciton density near the surface of the ZnSe layer. According to the energy-level diagram (Fig. 6), charge separation could occur at the organic/inorganic semiconductor interface at least in the case of 6T. For CN-3T it is hard to make predictions due to the uncertainty of the position of the LUMO level. A charge transfer process should manifest itself in changes of the PL yield of the heterostructure. Figure 7 displays the PL spectrum of 6T on ZnSe recorded at 5 K. The nominal layer thickness is 1.6 nm. The substrate was held at 373 K during the deposition of 6T. According to the AFM data [Fig. 1(a)], this corresponds to less than one monolayer of standing 6T molecules. The sample was excited at 465 nm, i.e., well below the band-gap energy of ZnSe, as above-band-gap excitation leads to an overlap of the 6T spectrum by spurious emission from deep centers of the ZnSe epilayer. The depicted spec-

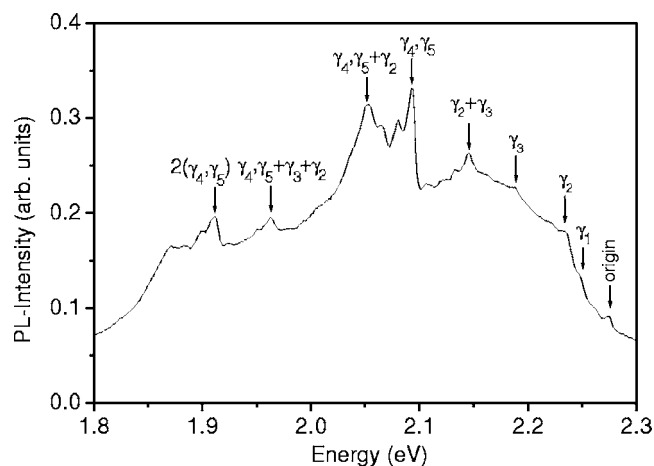


FIG. 7. PL spectrum recorded at 5 K of a thin layer (1.6 nm) of 6T deposited on ZnSe(100) at a substrate temperature of 373 K. The sample was excited at 465 nm. The 0-0 line and the most prominent vibronic lines are assigned.

trum comprises therefore only PL features of 6T. The origin of the PL spectrum of 6T lies at 2.274 eV as in the 6T single crystal. The vibronic lines are well resolved and can be assigned to five fundamental vibrational modes (ν_1 – ν_5) and their combinations.^{26,27}

As the spectrum resembles that of the 6T single crystal we can conclude that the arrangement of the molecules in the first monolayer should be very similar. The spectrum is superimposed on a broader background due to some degree of orientational disorder in the layer.²⁸

Due to the LUMO-CBM energy offset of 0.54 eV, an electron could be transferred from the excited molecule into the conduction band of the semiconductor at the ZnSe/6T interface which would lead to a quenching of the 6T luminescence. As the luminescence yield depends also on the structural order in the film, it cannot be decided from the present experimental data if there is some PL quenching due to charge transfer at the interface. However, as we do observe PL of the first monolayer, we can conclude that if charge transfer occurs, it should take place on a time scale comparable to or larger than the PL lifetime.

At first glance, our result is somewhat in contrast to that found in PL studies of quaterthiophene (4T) deposited on ZnSe(100).⁶ It was reported that the first two monolayers of 4T do not luminesce. The morphology of the investigated films was, however, very different from the samples reported here as a substrate temperature during the deposition of 20 K was chosen which resulted in 2–3 monolayers of flat-lying molecules. It was suggested that the luminescence quenching is due to a fast charge transfer process at the organic/inorganic interface which is, according to our photoemission data, possible. The LUMO-CBM energy offset could be even larger at the 4T/ZnSe interface as the HOMO-LUMO gap increases with decreasing number of thiophene rings. There are two explanations for the discrepancy. First, charge transfer from excited oligothiophenes should be more likely in the case of flat-lying molecules as compared to standing molecules. Second, in Ref. 4, the heterostructures were excited above the band gap of ZnSe. Also in our experiment, PL of 6T was hardly detectable under such excitation conditions due to the mentioned overlap of the spectrum by deep-level emission of ZnSe. This is due to the huge difference of the excited volume: less than one monolayer of 6T compared to the penetration depth of light in ZnSe which is approximately 150 nm. Therefore there might be also some residual PL of 4T at the ZnSe/4T interface in Ref. 6.

In Fig. 8, a PL spectrum of a 3-nm-thick CN-3T film deposited at 293 K on ZnSe is depicted. The excitation was again below the band gap of ZnSe. Even at low temperature (i.e., 8 K), the spectrum is very broad. As single crystals of CN-3T were too small and fragile to be mounted in a cryostat, a PL spectrum of CN-3T polycrystalline powder was measured for comparison. As expected, the spectra are very similar apart from a small shift and an additional shoulder at the high-energy side not resolved in the thin film spectrum. Due to the 3D nature of the film, the PL properties of CN-3T should not be influenced by the ZnSe surface as the largest fraction of the molecules is not in contact with the semiconductor. The large linewidths may be due to structural disorder.

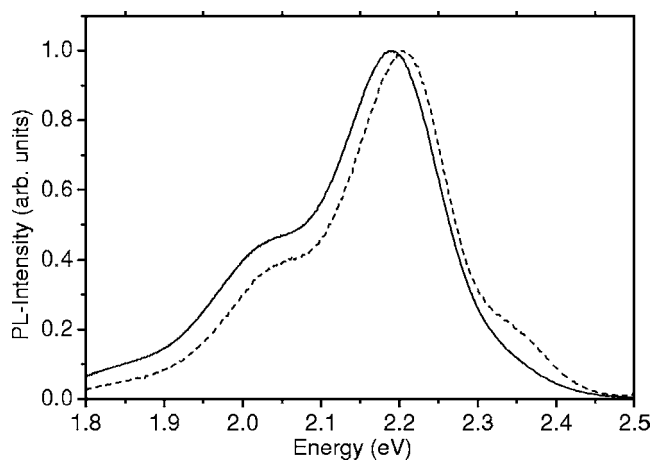


FIG. 8. PL spectra recorded at 8 K of a 3-nm-thick CN-3T film deposited on ZnSe(100) (solid line) and of CN-3T powder (dashed line). The substrate temperature during the growth of CN-3T on ZnSe was held at 298 K. The samples were excited at 461 (thin film) and 435 nm (powder).

SUMMARY AND CONCLUSIONS

On the $c(2 \times 2)$ reconstructed ZnSe(100) surface, 6T layers grow in a Stranski-Krastanov growth mode. Within a layer, the molecules stand upright, i.e., the contact plane is the (001) crystal plane. This growth mode is typically found for 6T on weakly interacting substrates where intermolecular interactions are stronger than the substrate-adsorbate interaction. The film morphology of CN-3T on ZnSe(100) is quite different. AFM data reveal that the organic layer is composed of 3D isolated crystallites or clusters. Photoemission data suggest that in between the clusters a wetting layer must be present.

Valence and core-level photoemission spectra show that the interface electronic structures of both 6T/ZnSe and CN-3T/ZnSe remain unperturbed, i.e., no hint at band bending or modification of the electronic structure of the deposited molecules due to formation of bonds with charge transfer with ZnSe surface atoms is found. This implies that the organic adlayer is bonded by van der Waals forces to the surface. The $c(2 \times 2)$ reconstructed ZnSe surface can therefore be considered as a chemically relatively inert surface. This is also reflected by PL measurements. Luminescence of the first monolayer of 6T on ZnSe could be observed and resembles that of the single crystal. It could not be decided from the present experiment whether some quenching of the PL occurs due to electron transfer from the excited molecules in the conduction band of the inorganic semiconductor occurs. However, according to the position of the respective energy levels, this process could in principle be possible. Also the PL properties of CN-3T are not influenced by the ZnSe surface which is in this case expected due to the 3D clustering of the organic film.

In conclusion, in contrast to other semiconductors, surface passivation of ZnSe $c(2 \times 2)$ is not needed to allow for an unperturbed and ordered growth of the organic adlayer if a

suitable molecule is chosen. This is a prerequisite for the realization of organic/inorganic hybrid structures where charge or electronic energy transfer processes at the interface shall be exploited. The soft lattice of ZnSe can set a limitation when aiming at commercial, long-term operating devices. It will be thus interesting to transfer the concepts

elaborated in this study to other II-VI compounds, e.g., ZnO and related materials.

ACKNOWLEDGMENT

This work was funded by the DFG in the frame of Sfb 448.

-
- ¹*Organic Light-Emitting Devices: A Survey*, edited by J. Shinar (Springer-Verlag, New York, 2004).
- ²*Organic Photovoltaics: Concepts and Realization*, edited by C. Brabec, V. Dyakonov, J. Parisi, and S. Sariciftci, Springer Series in Materials Science (Springer, Berlin, 2003).
- ³Y. Hirose, S. R. Forrest, and A. Kahn, *Phys. Rev. B* **52**, 14040 (1995).
- ⁴N. Nicoara, I. Cerrillo, D. Xueming, J. M. García, B. García, C. Gómez-Navarro, J. Méndez, and A. M. Baró, *Nanotechnology* **13**, 352 (2002).
- ⁵M. Kramer and V. Hoffmann, *Opt. Mater.* **9**, 65 (1998).
- ⁶M. Schneider, E. Umbach, A. Langner, and M. Sokolowski, *J. Lumin.* **111**, 275 (2004).
- ⁷*Handbook of Oligo- and Polythiophenes*, edited by D. Fichou (Wiley-VCH, Weinheim, 1999).
- ⁸J. Reichow, J. Griesche, N. Hoffmann, C. Muggelberg, H. Rossmann, L. Wilde, F. Henneberger, and K. Jacobs, *J. Cryst. Growth* **131**, 277 (1993).
- ⁹A. Yassar, F. Demanze, A. Jaafari, M. El Idrissi, and C. Coupry, *Adv. Funct. Mater.* **12**, 699 (2002).
- ¹⁰G. Horowitz, B. Bachet, A. Yassar, P. Lang, F. Demanze, J.-L. Fave, and F. Garnier, *Chem. Mater.* **7**, 1337 (1995).
- ¹¹R. Garcia and M. Tello, *Nano Lett.* **4**, 1115 (2004).
- ¹²A. J. Lovinger, D. D. Davis, R. Ruel, L. Torsi, A. Dodabalapur, and H. E. Katz, *J. Mater. Res.* **10**, 2958 (1995).
- ¹³P. Ostojica, S. Guerri, S. Rossini, M. Severidori, C. Taliani, and R. Zamboni, *Synth. Met.* **54**, 447 (1993).
- ¹⁴M. A. Loi, E. Da Como, F. Dinelli, M. Murgia, R. Zamboni, F. Biscarini, and M. Muccini, *Nat. Mater.* **4**, 81 (2005).
- ¹⁵J. E. Northrup, M. L. Tiago, and S. G. Louie, *Phys. Rev. B* **66**, 121404(R) (2002).
- ¹⁶I. G. Hill, A. Kahn, Z. G. Soos, and R. A. Pascal, *Chem. Phys. Lett.* **327**, 181 (2000).
- ¹⁷Z. Chen, D. Eich, G. Reuscher, A. Waag, R. Fink, and E. Umbach, *Phys. Rev. B* **60**, 8915 (1999).
- ¹⁸W. Chen, A. Kahn, P. Soukiassian, P. S. Mangat, J. Gaines, C. Ponzoni, and D. Olego, *Phys. Rev. B* **51**, 14265 (1995).
- ¹⁹F. Xu, M. Vos, J. H. Weaver, and H. Cheng, *Phys. Rev. B* **38**, 13418 (1988).
- ²⁰W. Chen, A. Kahn, P. Soukiassian, P. S. Mangat, J. Gaines, C. Ponzoni, and D. Olego, *Phys. Rev. B* **49**, R10790 (1994).
- ²¹M. J. Frisch *et al.*, GAUSSIAN 01, Gaussian, Inc., Pittsburgh, PA, 2001.
- ²²H. Ishii, K. Sugiyama, E. Ito, and K. Seki, *Adv. Mater. (Weinheim, Ger.) (Weinheim, Ger.)* **11**, 605 (1999).
- ²³A. Kahn, N. Koch, and W. Gao, *J. Polym. Sci., Part B: Polym. Phys.* **41**, 2529 (2003).
- ²⁴W. Weigand, A. Müller, L. Kilian, T. Schallenberg, P. Bach, G. Schmidt, L. W. Molenkamp, O. Bunk, R. L. Johnson, C. Kumpf, and E. Umbach, *Phys. Rev. B* **68**, 241314(R) (2003).
- ²⁵G. Hughes, J. Roche, D. Carty, T. Cafolla, and K. E. Smith, *J. Vac. Sci. Technol. B* **20**, 1620 (2002).
- ²⁶M. Schneider, M. Brinkmann, M. Muccini, F. Biscarini, C. Taliani, W. Gebauer, M. Sokolowski, and E. Umbach, *Chem. Phys.* **285**, 345 (2002).
- ²⁷M. Muccini, E. Lunedei, A. Bree, G. Horowitz, F. Garnier, and C. Taliani, *J. Chem. Phys.* **108**, 7327 (1998).
- ²⁸F. Meinardi, M. Cerminara, S. Blumstengel, A. Sassella, A. Borghesi, and R. Tubino, *Phys. Rev. B* **67**, 184205 (2003).